Available online at www.sciencedirect.com
ScienceDirect
Journal of Pharmaceutical and Biomedical Analysis 45 (2007) 382–389
JOURNAL OF PHARMACEUTICAL AND BIOMEDICAL ANALYSIS
www.elsevier.com/locate/jpba

Limits of a localized magnetic resonance spectroscopy assay for *ex vivo* myocardial triacylglycerol

Robert D. O'Connor [a], Robert J. Gropler [a], Linda Peterson [b], Jean Schaffer [c,d], Joseph J.H. Ackerman [a,d,e,*]

[a] *Department of Radiology, Washington University, Saint Louis, MO 63110, USA*
[b] *Department of Internal Medicine, Division of Cardiology, Washington University, Saint Louis, MO 63110, USA*
[c] *Center for Cardiovascular Research, Washington University, Saint Louis, MO 63110, USA*
[d] *Department of Internal Medicine, Washington University, Saint Louis, MO 63110, USA*
[e] *Department of Chemistry, Washington University, Saint Louis, MO 63110, USA*

Received 9 March 2007; received in revised form 27 August 2007; accepted 29 August 2007
Available online 1 September 2007

Abstract

Localized magnetic resonance spectroscopy (LMRS) promises a powerful non-invasive means to determine myocardial triacylglycerol (TAG) in a clinical setting. Here, the linearity, specificity, robustness, precision, and accuracy of an *ex vivo* mouse-heart LMRS TAG assay are assessed by quantifying the spatial, spectral, and relaxation-induced uncertainties. The protocol, which is based on localization by adiabatic selective refocusing (LASER) using frequency offset corrected inversion (FOCI) pulses, alternating gradient polarity, and simple post-processing, is shown to have good characteristics. The presented protocol has a benchmark, phantom-based, accuracy of 3%, and when applied to *ex vivo* mouse hearts the accuracy is 6%, making the LMRS assay comparable to the typical destructive bioanalytical assay.

Keywords: Quantitative localized MRS; LASER; FOCI; Triacylglycerol; Myocardial TAG; T_2 relaxation

1. Introduction

Accurate, non-invasive, *in vivo* assays are paramount to understanding and diagnosing disease. Localized magnetic resonance spectroscopy (LMRS), which uses gradient-enabled imaging systems, is increasingly used both in basic and clinical assays including qualitative and quantitative compositional, temperature, and pH measurements [1–15]. Kreis [16] summarized the main aspects of LMRS, including spectral artifacts, systematic errors, and general criteria for ensuring spectral quality. Jansen et al. [6] discussed important aspects of quantitative *in vivo* LMRS. Typically, LMRS validation studies report a coefficient of variation (CV) around 10%, with the best ranging roughly from 2 to 5%. These values are below the FDA recommendation of 15% [17], but the inconsistently achieved low CV's, more technical setup, and often complex data analysis that characterize LMRS pose challenges to its use as a clinically accessible diagnostic tool [18]. Nevertheless, LMRS is still one of the best options with regard to non-invasive, *in vivo* biological assays.

The overall goal of this research is to develop an *in vivo*, clinically accessible LMRS assay for myocardial triacylglycerol (TAG), the accumulation and metabolism of which has been linked to the pathogenesis of the cardiac dysfunction associated with a variety of diseases such as obesity and diabetes Mellitus [19–22]. Boesch et al. recently reviewed LMRS as applied to muscular TAG [3]. Generally, to be clinically accessible and useful for monitoring the efficacy of interventions, the assay must be straightforward to implement and the results easy to interpret with an overall accuracy (defined below) of roughly 10%. Noting these criteria, the ^{1}H LMRS technique employed here is based on simple post-processing and localization by adiabatic selective refocusing (LASER), a robust, precise, and clinically amenable localization method [7,23–25]. The development of the TAG assay is proceeding in two stages: first, implementation

* Corresponding author at: Department of Radiology, Washington University, Saint Louis, MO 63110, USA. Tel.: +1 314 935 6593; fax: +1 314 935 4481.
E-mail address: ackerman@wustl.edu (J.J.H. Ackerman).

0731-7085/$ – see front matter © 2007 Elsevier B.V. All rights reserved.
doi:10.1016/j.jpba.2007.08.022

and validation in phantom and *ex vivo* studies, and second, implementation *in vivo*. Because the precision of the second *in vivo* stage will be degraded by cardiac and respiratory motion [4,26], the targeted precision for the first stage is ~5%.

The first stage, which is reported here, first characterizes the limitations of the LMRS TAG protocol using on a 4.7 T small-animal MR scanner and multi-compartment phantoms. The characterization proceeds by optimizing the critical parameters of the protocol and quantifying the effects of these parameters, and that of T_2 relaxation, on the measurement uncertainty. The well resolved ^{1}H resonances, uniform magnetic susceptibility, long relaxation times, and precise analyte containment of the phantoms allow for a clear characterization of the detrimental effects that localization has on the assay. After this characterization, the phantom-optimized protocol is applied to *ex vivo* mouse hearts, and the results compared to biochemical analysis. The *ex vivo* mouse-heart samples have broader, multiple component ^{1}H resonances, short relaxation times, and are typical of what can be expected of *in vivo* TAG assays, though without the additional challenge of sample motion.

2. Experimental

2.1. Phantom samples

Phantoms consisted of sealed 1.2 mm i.d. polypropylene tubes that were filled with gravimetrically prepared dilutions of *t*-butanol in distilled H_2O and placed together in an H_2O medium. Assay voxels were localized entirely within each respective tube with approximate dimensions of 1 mm × 1 mm × 4 mm. Generally, six spectra for each concentration were collected at different times over a period of 6 months. For parameter testing, six variations were typically acquired serially. Bulk *t*-butanol/H_2O or acetone/H_2O phantoms were also used in various tests. All phantom spectra were collected at 20 ± 2 °C.

2.2. Ex vivo mouse-heart samples

Ex vivo mouse-heart samples were obtained from transgenic MHC-ACS mice which have cardiac-specific overexpression of long-chain acyl-CoA synthetase, an enzyme that contributes to FFA transport by vectorial acylation and/or metabolic trapping [20]. These mice exhibit a metabolic cardiomyopathy characterized by TAG accumulation that is associated with cardiac myocyte apoptosis, left ventricular systolic dysfunction, and premature death. These transgenic mice and their wild type littermates, both of which were either fed or 24 h starved, provided a wide range of myocardial TAG levels. The *ex vivo* hearts were prepared by perfusion fixation with 10% formamid, excising, and quenching in liquid N_2. The samples were then placed adjacent to a sealed, limited-volume, 0.02%-^{1}H *t*-butanol reference standard that was in a 3 cm^3 plastic syringe filled with D_2O. The MR voxels, with dimensions of approximately 3 mm × 3 mm × 6 mm, encompassed the *entire* heart or the *entire* volume of the reference standard, as appropriate.

Quantitative *ex vivo* spectra were acquired at 37 ± 5 °C and then the samples were again frozen in liquid N_2, stored at −20 °C for at most 4 h, and then stored at −80 °C for at most 1 week, at which point TAG was extracted twice and biochemically analyzed [27–29]. Based on lipid analysis, values of 85 and 77 ^{1}H's per TAG molecule were used for the MRS wild type and mutant MRS TAG calculations, respectively [20]. The *ex vivo* spectra were collected over a 2-month period. Three serial repetitions were acquired from three samples to verify the reproducibility and precision results obtained from the phantoms.

2.3. Localized magnetic resonance spectroscopy

The MR scanner consisted of an Oxford Instruments' (Oxford, UK) 200/400 (4.7-T = B_0: 200 MHz, 40-cm clear bore) magnet, a 10-cm inner diameter actively shielded Magnex (Oxford, UK) gradient coil (~60 G/cm, ~200 μs rise time), Crown/Techron (Elkhart, IN, USA) gradient power supplies, a Stark Contrast (Erlangen, Germany) 2.5 cm birdcage coil, and a Varian NMR Systems (Palo Alto, CA, USA) UNITY-*INOVA* console.

The pulse sequence, which employs frequency offset corrected inversion (FOCI) pulses, is depicted in Fig. 1. A more detailed technical description of the LMRS protocol, including the LASER-FOCI sequence, acquisition parameters, and post-processing is in Appendix I of the supplementary material. Generally, phantom spectra were acquired partially relaxed at a single T_e point (30 ms) and *ex vivo* spectra were acquired essentially fully relaxed at two T_e points (30 and 55 ms). The post-processing was straightforward and consisted of zero-filling, apodization, Fourier transforming, manual zero-order phasing, and, finally, macro-driven automatic integration.

3. Results

3.1. Pulse sequence/gradients/localization

To minimize spectral distortions, the protocol requires optimized gradient and sequence parameters (Appendix I), such that simple alternation of the gradient polarity on every scan effectively eliminates modulations from acoustic ringing [30]. As can be seen in Fig. 2, the gradient acoustic ringing induced signals are not perfectly cancelled by alternating the gradient polarity (top spectrum), but their intensity is reduced by a factor of 10. Overall, alternating the gradient polarity decreases the artifacts to below 1% that of the average TAG resonance for a 30 ms T_e.

Once spectral distortions are eliminated, the accuracy and specificity of localization are ultimately characterized by the amount of outer volume (OV) contamination. The three main sources of OV contamination are chemical shift displacement, non-ideal π-pulse refocusing characteristics, and non-ideal pulse spatial profiles. The large bandwidth, sharp frequency transition, and generally excellent inversion profile of the FOCI pulses, along with alternating gradients, phase cycling, and crushers, minimize this contamination. A plot of the cube-root of the voxel volume *versus* the cube-root of the integrated area for effective bandwidths between 4 and 20k has slope of 1.013, intercept of −0.03, and a Pearson product–moment correlation (PPMC) of 0.999. This correlation demonstrates the overall

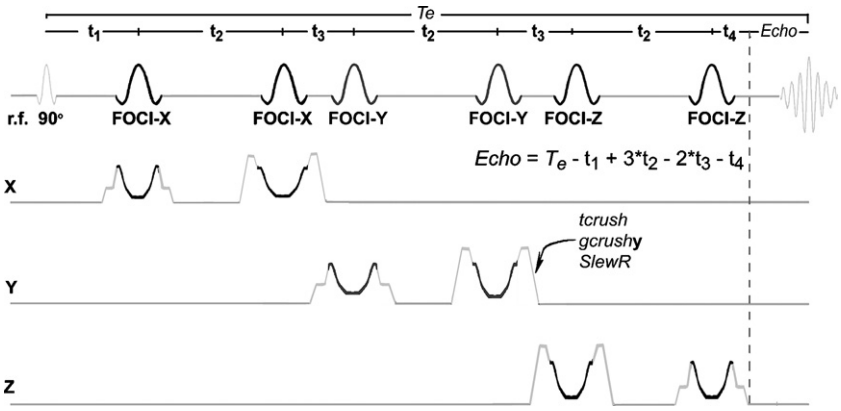

Fig. 1. The LASER-FOCI pulse sequence. The r.f. and gradient waveforms are generated according to Eqs. (A1)–(A5) of the supplementary material. The parameter *Echo* defines the time between the gradients being off and data acquisition.

excellent accuracy and robustness of the localization. However, the 1.013 slope and minor differences between the 4k and higher bandwidth data sets are consistent with a small amount of OV contamination [16,31,32].

Fig. 3 shows spectra from a voxel that was placed inside of an empty tube, and demonstrates the absolute accuracy of localization, which is about 0.2 mm based on the signal present following incremental increases in the size of the "empty" voxel. Thus, to minimize partial/outer volume contamination, as in the top spectrum of Fig. 3, the volume of interest (VOI) should be kept 0.2 mm away from regions that are not of interest.

3.2. Relaxation

The propagation of errors analysis in Appendix II of the supplementary material addresses three pertinent LMRS experiments and their requisite relaxation correction: a single-T_e acquisition and correction *via* literature-assumed T_2 parameters, similar to our phantom measurements; a two-T_e point acquisition with extrapolation to $T_e = 0$; and, a two-T_e point acquisition with an external reference, which is our *ex vivo* TAG protocol. Typical LMRS assays use the first, single-T_e method, acquiring one spectrum and using T_2 values from the literature to correct for relaxation. For this method and T_2 parameters taken from the literature [9], the *ex vivo* TAG assay would have a CV of at least 6%. However, because there is minimal loss of precision with this and other methods if $T_e \ll T_2$, this method adds only 0.7% to the overall CV of the phantom assays where T_2 is long.

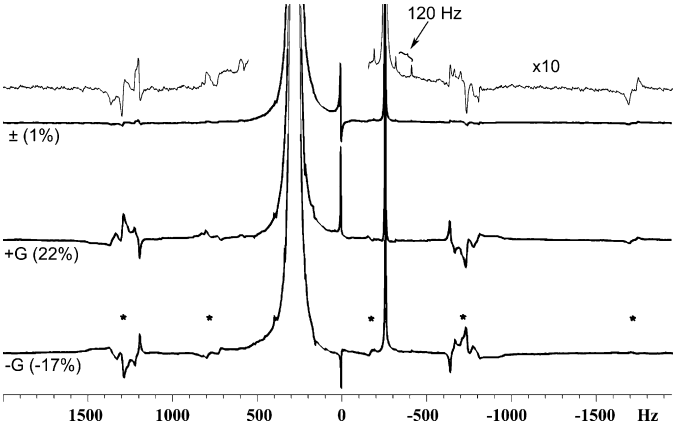

Fig. 2. Gradient acoustic ringing-induced signals (0.7 [%^{1}H] acetone/H_2O phantom). The bottom and middle spectra were acquired with the LASER-FOCI protocol except for using only negative and positive gradient polarity, respectively. The pairs of signals at −200/800, −700/1300, and −1700/2300, denoted with asterisks, result from a 500 Hz acoustic modulation of the H_2O signal. The top spectrum was acquired with the full protocol, *i.e.* the gradient polarity alternates every scan. Gradient power supply signals are also visible in the expanded ± spectrum around the acetone resonance at −250 Hz. The numbers on the left represent the differences between the LMRS and gravimetric acetone/H_2O ratio.

The second method estimates T_2 values directly and requires two spectra to be acquired, one at the shortest feasible T_e and the second at a T_e that depends on the SNR and T_2 values. In comparison to the first method, the two-T_e point extrapolation method is more precise and, considering potential tissue heterogeneity [6,33], more robust. The calculated CV for this type of *ex vivo* TAG assay is 4–5%.

The *ex vivo* protocol of the present work uses an external reference because void volumes, sample heterogeneity, and D_2O exchange over the time scale of the assay interfere with employing internal tissue H_2O as a reference. This method is a hybrid of the first two methods and requires a single-T_e spectrum of the reference and two analyte spectra at different T_e's. With this method, the calculated CV for the *ex vivo* TAG assay is 5.3%. It should be mentioned that, as a result of B_1 heterogeneity, the external reference method may not be viable without adiabatic pulses.

3.3. Linearity

Linearity defines the spectrometer response to changing signal, which for localized spectroscopy is a function of both voxel size and concentration. With regard to voxel volume, the volume/intensity correlation and Fig. 3 suggest that the adiabatic sequence correctly assays the voxel. With regard to concentration, the linearity of the MRS response to the number of nuclei is well documented [34,35]. The LMRS response of the protocol is the relaxation corrected analyte-to-reference ratio of

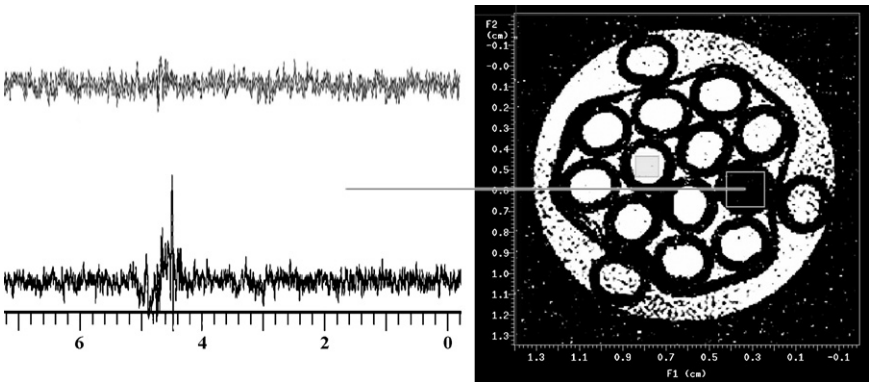

Fig. 3. The image is a spin-echo slice of a phantom composed of tubes of various concentrations of *t*-butanol in H_2O. The spectra to the left were acquired with the LMRS protocol and localized to the empty voxel. The small signals demonstrate the accuracy and robustness of the adiabatic pulses, in general, and suggest a localization accuracy of about 0.2 mm (based on small changes to the voxel size). The lower spectrum was acquired with $f = 1$, $bw = 7.7$ kHz and no alternating gradients. The upper spectrum was acquired with $f = 13$, $bw = 1$ kHz and alternating gradients. The small gray rectangle to the left of the empty voxel is a representative voxel for the *t*-butanol data.

the integrated intensities, S_0. For the range 0.7–20% populated with 11 standards, the gravimetric *versus* LMRS measurement of the percent ^{1}H in mixtures of *t*-butanol and H_2O has a slope of 0.993 ± 0.012, a negligible intercept, and a PPMC of 1.0 ($n = 63$ measurements). For the *ex vivo* LMRS TAG protocol *versus* the enzymatic assay, the slope is 0.96 ± 0.1 with an intercept of 0.0043 ± 0.013 and a PPMC of 0.99 ($n = 17$). All confidence intervals are at the 95% level. The increased uncertainty in the *ex vivo* TAG assay compared to the phantom likely results from both increased line widths and uncertainty in the lipid extraction and bioassay, which is roughly 10% [28,29].

Table 1
The essential parameters, limits, protocol value, and CV of the LMRS protocol

Parameter	Effect	Limits	Protocol value	CV
Robustness				
Gradients	Integration	<39 G/cm	Alternating	≈1%
SlewR	*Echo*, min T_e	<150k G/(cm s)	125k	
Echo	Integration	>1.75 ms	2.5 ms	
pw_π	Min T_e, SS, SNR	>2.25 ms	3.25 ms	
$B^0_{1,180}$	Min T_e, SNR	±1 kHz	3.0 kHz	<0.1%
$B^0_{1,90}$	SNR	±500 Hz	4.17 kHz	<0.2%
pos	SNR	90% of center		<0.2%
Selectivity				
*tcrush*n	OV, T_e	>200 μs	300 μs	
*gcrush*n	OV, T_e	$8 < x < 24$	24_x, 20_y, 16_z	
Effective *bw* ($f \cdot bw$)	SS	>12k	>12k	
FWHM (H_2O)	CS		<40 Hz	
vox (1 dimension)	SNR, SS	>0.5 mm	>0.8 mm	<0.1%
Precision				
Line broadening	CS, SNR	5–15 Hz	5 Hz Gaussian	
Scans (*NT*)	SNR, integration	≥32	32, 128, 256	
SNR	Integration	>30	≈75	<1%
Accuracy				
T_e	SNR, CS, RC, S.Er	>28 ms	30, 55 ms	
tof		±100 Hz	3 ppm	<0.5%
Excitation pulse	SNR, *Tr*	Adiabatic/hard	90° hard	0.7%
Phasing	Integration			<0.2%
H_2O integration		>±20 FWHM	Auto	<1%
t-Butanol integration		±10 FWHM	Auto	1.5%
TAG integration		0.6–1.9 ppm	Auto	2%
Tr TAG	≈95% relaxed		4 s	<0.5%
Tr standard	≈50% relaxed, S.Er		1.5 s	1%

S.Er: systematic error (bias); CS: chemical selectivity; SS: spatial selectivity; RC: T_2 relaxation correction; auto refers to the macro-driven automatic integration. See Appendix I in the supplementary material for parameter definitions.

3.4. Robustness/ruggedness

The robustness and ruggedness of the assay characterizes the general dependence of the CV on reasonable parameter changes including those of the spectrometer and operator. Based on phantom measurements, Table 1 lists the main parameters, their primary impact, limits, protocol value, and CV when applicable. These parameter CV's, CV_p, were estimated by varying the applicable parameter(s) within the prescribed limits and subtracting a base CV of 2% from the observed CV, CV_{obs}, Eq. (1). The measured quantity was the analyte-to-reference ratio, S, and 2% is the average CV of S, CV_S, from all the phantom measurements in the primary study

$$CV_p = \sqrt{CV_{obs}^2 - 0.02^2} \quad (1)$$

For example, the *gradient* CV represents the variation in S as a result of varying *Echo*, *SlewR*, and *gcrush*n within their prescribed limits. The parameters are grouped into the categories which they affect the most, but most parameters have multiple effects. Operator and spectrometer dependencies were not specifically investigated, but the parameter variations are representative of changing operators.

For LMRS, robustness primarily pertains to localization, acquisition, processing, and sample. The localization itself is spatially very robust, and changing the position or size of the voxel does not affect CV_S. Only with parameters outside the protocol limits, or with extremely poor shimming, can signals originating from regions external to the VOI be observed. As for acquisition and processing, the CV's and limits of the parameters generally suggest a very robust assay. The main detractor is the strong dependence of the assay CV on the minimum T_e, which is spectrometer specific and for which the effect can be estimated *via* the relaxation analysis.

Concerning the *ex vivo* samples, the assay is robust as long as the H_2O ^1H line width is below 40 Hz. CV_S deteriorates quickly as the full width at half maximum (FWHM) exceeds 40 Hz, a limit that is directly proportional to B_0. Additionally, Fig. 4 indicates that the assay is relatively independent of the temperature and time at which the fixed myocardium assay occurs, though an elevated temperature is preferable due to the decreased line width. However, significant TAG decomposition (10%) does occur with *ex vivo* myocardium after 4 h at 35 °C.

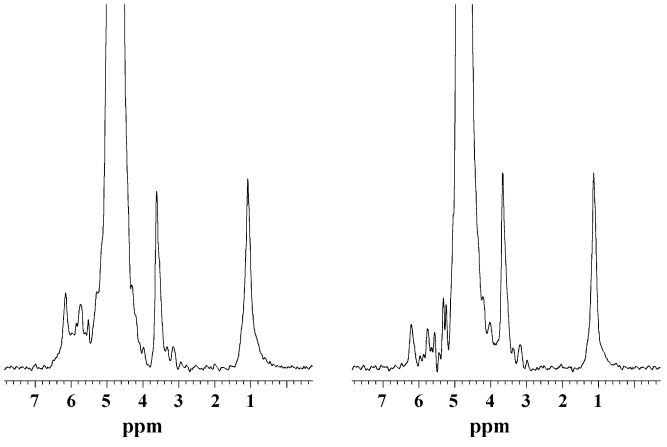

Fig. 4. LASER-FOCI spectra of *ex vivo* mouse hearts taken at 20 °C immediately after excision (left) and after equilibrating at 35 °C for 1 h (right). The TAG resonance at ≈1 ppm is only 0.5% smaller on the right.

3.5. Selectivity/specificity

The assay does not distinguish between intra- (IMCL, 1.3 ppm) or extra-myocellular (EMCL, 1.4 ppm) TAG, nor the various species of fatty acids [2,3,9]. Thus, assuming that the VOI can always be located 0.2 mm from non-targeted tissue regions, the selectivity and specificity of the TAG assay reduce to registering all the TAG and to discerning the alkyl and methyl resonances of TAG from those of the vast number of other species, which are roughly 1% that of TAG [9,36]. The LMRS *versus* enzymatic intercept of 0.004 suggests that other resonances are indeed unimportant. Based on the corresponding slope, though, there are discrepancies with the bioassay.

3.6. Reproducibility/repeatability

Reproducibility was verified by repeated phantom acquisitions over a period of 6 months, with an overall CV_S of 2%. Serially repeated acquisitions would typically yield a CV_S of less than 1.5%. Similarly, serially repeated acquisitions of *ex vivo* samples had a CV_S of 2%.

4. Discussion

4.1. Pulse sequence/gradients/localization

The general characteristics of the alternating gradient-polarity LASER-FOCI sequence (minimal calibration, insensitivity to r.f.-magnetic field (B_1) inhomogeneities and acoustic noise, large bandwidths, and sharp frequency transitions) provide an accurate, robust, and clinically accessible assay by minimizing operator, sample, and spectrometer dependencies. Additionally, the increased SNR [24] that results from the excellent inversion profile of the FOCI pulses compensates for much of the accuracy that is lost as a result of the longer T_e's and larger relaxation correction.

4.2. Relaxation

Although a limit-based error analysis of the relaxation correction has been published [37], many studies report CV's based only on repeated acquisitions and do not include the uncertainty of the T_2 correction [5,8,9,12]. For species with comparatively long T_2's, such as brain metabolites, the additional uncertainty is minor. For short-T_e TAG assays using literature T_2 values, the correction adds approximately 4% to the base CV, but it becomes more significant with increasing T_e [38]. The simple propagation of errors analysis presented in Appendix II provides an easy transfer from measured CV_S to the assay CV. It also gives insight into optimal experiment design [39–41].

It should also be noted that, though a reasonable first approximation at short T_e values, the relaxation profiles for lipids and

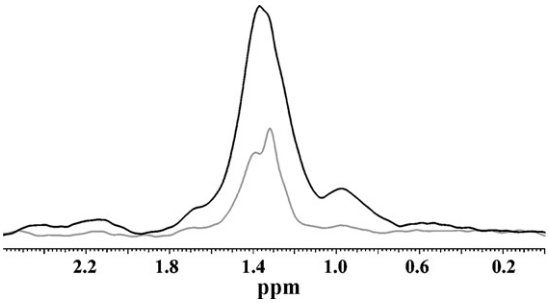

Fig. 5. LASER-FOCI *ex vivo* myocardium TAG resonance with $T_e = 30$ ms (black) and 75 ms (gray).

intercellular H_2O are not purely exponential. Considering the range from 0.6 to 1.9 ppm, which includes both CH_2 and CH_3 moieties and both IMCL and EMCL lipid, this approximation is obviously inaccurate, as the T_e-dependent line shape shown in Fig. 5 demonstrates. The exponential approximation to the relaxation correction will result in a systematic error and decreased precision, but for short T_e's and a relatively narrow distribution of T_2's this error is minor compared to other uncertainties.

4.3. Selectivity/specificity

The discrepancy with the bioassay (slope = 0.96) may result from some TAG being immobile and thus "MR invisible" [3]. Although there are undoubtedly some alkyl and methyl TAG moieties that are not reporting, the similarity between ambient and elevated temperature spectra shown in Fig. 4 suggests that the immobile, non-reporting fraction is small. On the other hand, the enzymatic bioassay is not explicitly specific for TAG, and could be counting phospholipids, which account for 5–7% of the lipid pool [42,43]. The ^{1}H/TAG ratio or a systematic error from the relaxation correction could also cause the discrepancy. It should also be noted that the heterogeneous relaxation biases the TAG morphological specificity, Fig. 5, and has been used to separate the IMCL and EMCL resonances [3,38].

4.4. Precision

Precision is a measure of the overall variability of an assay. For LMRS, the precision can be divided into spatial, relaxation, and integration components, of which the spatial and relaxation have already been discussed. Because phasing of the complex data is straight forward in echo spectroscopy, the integration component of the assay primarily depends on baseline distortions and line width, of which major baseline distortions are minimized by alternating the gradient polarity. More general baseline and integration-limit problems stem from the merging of relatively broad line shapes that result from the inhomogeneous B_0 and large reference-to-analyte ratios.

The phantom resonances have relatively narrow line widths and require minimal relaxation corrections. Thus, they allow the inherent loss of precision from the above factors to be estimated. For the phantoms, and based on serially repeated processing, the macro-driven integration of the H_2O ^{1}H resonance has a CV less than 1.0% once the limits are greater than ±20 FWHM. For the *t*-butanol resonance, the limits that result in the smallest CV are smaller (±10 FWHM), and the CV for the integration is roughly 1.5%. The smaller limits result from the *t*-butanol resonance residing on a wing of the H_2O resonance, making baseline determination more difficult. These CV's are not concentration-dependent within the range studied (PPMC = −0.12). Consistent with these values $CV_S \approx 2\%$ and, with the relaxation correction, the CV for the *t*-butanol assay should be 2.6%, which represents the optimal for this protocol and spectrometer. Experimentally, the *t*-butanol CV for the relative difference between the predicted and gravimetric is 2.9%.

For the *ex vivo* TAG assay, the broad, multi-component resonance further exasperates definition of appropriate integration limits. Choosing an integration limit of 1.9 ppm, as opposed to 2.5 which would include the functionalized CH_2's, yields the most consistent results. Again, the smaller limits probably better approximate a straight baseline. The low frequency integration limit enclosing the methyl resonances is clear, though some intensity is undoubtedly missed as a result of the broad line width. For TAG, small variations of these limits and serial acquisitions suggest that the CV for the resonance area is 2%. Incorporating the hybrid relaxation correction, CV for the TAG assay should be around 5.3%, which is consistent with the 95% confidence level of the slope in the LMRS *versus* bioassay analysis.

4.5. Accuracy

The accuracy of the assay is defined as [35]:

$$\text{accuracy} = \sqrt{\text{CV}^2 + \text{bias}^2} \quad (2)$$

where bias is the difference between the slope of the experimentally determined correlation and an ideal slope of 1, true *versus* measured. Based on the phantoms, the accuracy for the basic LASER-FOCI protocol is 2.9%. For the *ex vivo* myocardium TAG assay with a CV of 5.3%, the accuracy of the protocol is 6.4%, which may be reduced by using a longer T_{e_2}.

Validation studies presenting both the precision and accuracy of an LMRS assay are rare, especially if these aspects of the localization are also considered. For comparison, CV's from repeated bulk phantom measurements, which do not address localization, typically range between 2 and 4% [13–15], with accuracies around 6% [13]. This accuracy would deteriorate rapidly if localization became critical because OV contamination can be high [32,44]. Considering the excellent localization properties of the LASER-FOCI sequence [24], as confirmed herein, the phantom results of the protocol compare well with other assays. Yet, the LMRS protocol is roughly three times less accurate than high-resolution, non-localized MRS assays [34,35]. Though some decrease in accuracy results from low analyte-to-reference ratios, it is primarily attributable to larger line widths and gradient-induced spectral noise, as is well known. Alternating the gradient polarity greatly decreases this noise for short-T_e protocols.

Concerning TAG MRS-to-biochemical comparisons, both an *ex vivo*, non-localized, high-resolution MRS study [45], which used an external standard, and several *in vivo* LMRS studies (fol-

lowed by biopsies) [9,46], which were based on internal tissue H_2O, report +0.9 correlations with slopes around 1. However, one report failed to show a correlation [47]. Typically, the LMRS assays report CV's from 6 to 10% based on repeated acquisitions [48,49] and do not directly address uncertainties involved with localization or relaxation. The LASER-FOCI based LMRS TAG protocol presented here has a comparable CV, but with the addition of incorporating most of the experimental uncertainties and verifying the quality of localization.

5. Conclusion

The protocol based on the LASER-FOCI sequence has precise localization, minimal operator intervention, and simple data processing, all of which serve to minimize the measurement uncertainty and maximize robustness. Based on the *t*-butanol results, the benchmark accuracy of the LASER-FOCI protocol is about 3%, which is roughly three times worse than that of traditional, non-localized analytical MRS. As a result of increased uncertainty due to relaxation and increased bias, the accuracy decreases to 6% for the *ex vivo* TAG assay. A two-T_e point assay would slightly increase the accuracy and potentially increase the robustness, too. These results place lower limits on the uncertainty of LMRS myocardial TAG analysis *in vivo*, where the challenges of cardiac motion and patient compliance will further degrade the assay. Finally, the *ex vivo* LMRS assay takes roughly 0.5 h per sample; requires no solvents and little preparation time; and, has an accuracy well below the FDA recommendation of 15%. Thus, it or similar MRS-based assays are attractive alternatives to biochemical methods [29,47,50].

Acknowledgements

The authors are grateful for helpful discussions with Dmitriy A. Yablonskiy and members of the Biomedical MR Laboratory. This work was supported, in part, by NIH grants P20 RR020643 and R24-CA83060 (Small Animal Imaging Resource Program).

Appendix I/II

Supplementary material associated with this article can be found, in the online version, at doi:10.1016/j.jpba.2007.08.022.

References

[1] A.M. Blamire, B. Rajagopalan, G.K. Radda, Magn. Reson. Med. 41 (1999) 198–203.
[2] C. Boesch, J. Décombaz, J. Slotboom, R. Kreis, Proc. Nutr. Soc. 58 (1999) 841–850.
[3] C. Boesch, J. Machann, P. Vermathen, F. Schick, NMR Biomed. 19 (2006) 968–988.
[4] J. Felblinger, B. Jung, J. Slotboom, C. Boesch, R. Kreis, Magn. Reson. Med. 42 (1999) 903–910.
[5] J.J.G. Geurts, F. Barkhof, J.A. Castelijns, B.M.J. Uitdehaag, C.H. Polman, P.J.W. Pouwels, J. Magn. Reson. Imaging 20 (2004) 366–371.
[6] J.F.A. Jansen, W.H. Backes, K. Nicolay, M.E. Kooi, Radiology 240 (2006) 318–332.
[7] M.N.E. Kassem, R. Bartha, Magn. Reson. Med. 49 (2003) 918–927.
[8] J.S. Reingold, J.M. McGavock, S. Kaka, T. Tillery, R.G. Victor, L.S. Szczepaniak, Am. J. Physiol. Endocrinol. Metab. 289 (2005) E935–E939.
[9] L.S. Szczepaniak, E.E. Babcock, F. Schick, R.L. Dobbins, A. Garg, D.K. Burns, J.D. McGarry, D.T. Stein, Am. J. Physiol. 276 (1999) E977–E989.
[10] R.W. vd Meer, S. Skozerke, J. Doornbos, M. Schär, J.J. Bax, A. de Roos, H.J. Lamb, J. Cardiovasc. Magn. Reson. 8 (2006) 102–103.
[11] W. Wlodarczyk, M. Hentschel, P. Wust, R. Noeskek, N. Hosten, H. Rinnebergk, R. Felix, Phys. Med. Biol. 44 (1999) 607–624.
[12] M. Kankäänpää, H.-R. Lehto, J.P. Pärkkä, M. Komu, A. Viljanen, E. Ferrannini, J. Knuuti, P. Nuutila, R. Parkkola, P. Iozzo, J. Clin. Endocrinol. Metab. 91 (2006) 4689–4695.
[13] A. Simmons, M. Smail, E. Moore, S.C.R. Williams, Magn. Reson. Imaging 16 (1998) 319–330.
[14] I. Hancu, S. Adak, E. Hutchison, R. Hurd, Proc. Int. Soc. Magn. Reson. Med. 11 (2004) 305.
[15] N. Sorenia, M.D. Noseworthy, T. Cormierb, W.K. Oakdene, S. Bells, R. Schachar, Magn. Reson. Imaging 24 (2006) 187–194.
[16] R. Kreis, NMR Biomed. 17 (2004) 361–381.
[17] FDA, Definitions and Terminology, March 1995.
[18] L. Gluch, ANZ J. Surg. 75 (2005) 464–470.
[19] M. Alavaikko, R. Elfving, E.J. Hirvonen, J. Jarvi, J. Clin. Pathol. 26 (1973) 285–293.
[20] H. Chiu, A. Kovacs, D. Ford, F. Hsu, R. Garcia, P. Herrero, J. Saffitz, J. Schaffer, J. Clin. Invest. 107 (2000) 813–822.
[21] B. Rodgrigues, M.C. Cam, J.H. McNeill, Mol. Cell. Biochem. 180 (1998) 53–57.
[22] A. Virkamäki, E. Korsheninnikova, A. Seppälä-Lindroos, S. Vehkavaara, T. Goto, J. Halavaara, A. Häkkinen, H. Yki-Järvinen, Diabetes 50 (2001) 2337–2343.
[23] M. Garwood, L. DelaBarre, J. Magn. Reson. 153 (2001) 155–177.
[24] P. Kinchesh, R.J. Ordidge, J. Magn. Reson. 175 (2005) 30–43.
[25] R.J. Ordidge, M. Wylezinska, J.W. Hugg, E. Butterworth, F. Franconi, Magn. Reson. Med. 36 (1996) 562–566.
[26] M. Schär, S. Kozerke, P. Boesiger, Magn. Reson. Med. 51 (2004) 1091–1095.
[27] Serum Triglyceride Determination Kit, TR0100, Sigma–Aldrich, St. Louis, MO 63103.
[28] S.J. Iverson, S.L. Lang, M.H. Cooper, Lipids 36 (2001) 1283–1287.
[29] S.K. Srivastava, S. Pradhan, B. Mittal, R. Kumar, G.A.N. Gowda, Anal. Lett. 39 (2006) 297–315.
[30] Z. Dong, W. Dreher, D. Leibfritz, Magn. Reson. Med. 55 (2006) 1441–1446.
[31] N.M. Yongbi, G.S. Payne, D.J. Collins, M.O. Leach, Phys. Med. Biol. 40 (1995) 1293–1303.
[32] I.M. Burtscher, E. Johansson, S. Holtås, F. Ståhlberg, Magn. Reson. Imaging 17 (1999) 1511–1519.
[33] L.L. Ploutz-Snyder, S. Nyren, T.G. Cooper, E.J. Potchen, R.A. Meyer, Magn. Reson. Med. 37 (1997) 676–682.
[34] F. Malz, H. Jancke, J. Pharm. Biomed. Anal. 38 (2005) 813–823.
[35] G. Maniara, K. Rajamoorthi, S. Rajan, G.W. Stokton, Anal. Chem. 70 (1998) 4921–4928.
[36] I. Mader, U. Seeger, R. Weissert, U. Klose, T. Naegele, A. Melms, W. Grodd, Brain 124 (2001) 953–961.
[37] F. Jírů, M. Dezortová, M. Burian, M. Hájek, Magn. Reson. Mater. Phys. Biol. Med. 16 (2003) 135–143.
[38] A. Škoch, F. Jírů, M. Dezortová, E. Krusinová, S. Kratochvílová, T. Pelikánová, W. Grodd, M. Hájek, J. Magn. Reson. Imaging 23 (2006) 728–735.
[39] G.F. Mason, G.M. Pohost, H.P. Hetherington, J. Magn. Reson. 107 (1995) 68–73.
[40] A. Narayanan, J.S. Hartman, A.D. Bain, J. Magn. Reson. 112 (1995) 58–65.
[41] R.I. Shrager, G.H. Weiss, R.G.S. Spencer, NMR Biomed. 11 (1998) 297–305.
[42] N. Griffon, E.C. Budreck, C.J. Long, U.C. Broedl, D.H.L. Marchadier, J.M. Glick, D.J. Rader, J. Lipid Res. 47 (2006) 1803–1811.
[43] M.G. McCoy, G.-S. Sun, D.H.L. Marchadier, C. Maugeais, J.M. Glick, D.J. Rader, J. Lipid Res. 43 (2002) 921–929.
[44] S.F. Keevil, M.C. Newbold, Magn. Reson. Imaging 19 (2001) 1217–1226.

[45] L.S. Szczepaniak, R.L. Dobbins, G.J. Metzger, G. Sartoni-D'Ambrosia, D. Arbique, W. Vongpatanasin, R. Unger, R.G. Victor, Magn. Reson. Med. 49 (2003) 417–423.
[46] J.R. Garbow, X. Lin, N. Sakata, Z. Chen, D. Koh, G. Schonfeld, J. Lipid Res. 45 (2004) 1364–1371.
[47] H. Howald, C. Boesch, R. Kreis, S. Matter, R. Billeter, B. Essen-Gustavsson, H. Hoppeler, J. Appl. Physiol. 92 (2002) 2264–2272.
[48] C. Boesch, H. Slotboom, H. Hoppeler, R. Kreis, Magn. Reson. Med. 37 (1997) 484–493.
[49] E.L. Thomas, G. Hamilton, N. Patel, R. O'Dwyer, C.J. Doré, R.D. Goldin, J.D. Bell, S.D. Taylor-Robinson, Gut 54 (2004) 122–127.
[50] M.W. McGowan, J.D. Artiss, D.R. Strandbergh, B. Zak, Clin. Chem. 29 (1983) 538–542.